Published in final edited form as:
Biomacromolecules. 2012 August 13; 13(8): 2333–2338. doi:10.1021/bm300578p.

Glycan-Targeted Virus-like Nanoparticles for Photodynamic Therapy

Jin-Kyu Rhee[1], **Michael Baksh**[1], **Corwin Nycholat**[2], **James C. Paulson**[2], **Hiroaki Kitagishi**[1,3,*], and **M.G. Finn**[1,*]

[1]Department of Chemistry, The Scripps Research Institute, 10550 North Torrey Pines Road, La Jolla, California 92037, USA

[2]Department of Chemical Physiology and Molecular Biology, The Scripps Research Institute, 10550 North Torrey Pines Road, La Jolla, California 92037, USA

[3]Department of Molecular Chemistry and Biochemistry, Faculty of Science and Engineering, Doshisha University, Kyotanabe, Kyoto 610-0321, Japan

Abstract

Virus-like particles (VLPs) have proven to be versatile platforms for chemical and functionalization for a variety of purposes in biomedicine, catalysis, and materials science. We here the simultaneous modification of the bacteriophage Qβ VLP with a metalloporphyrin derivative photodynamic therapy and a glycan ligand for specific targeting of cells bearing the CD-22 receptor. This application benefits from the presence of the targeting function and the delivery of a high local concentration of singlet oxygen-generating payload.

Keywords

Virus-like particles; photodynamic therapy; cell targeting

Introduction

Virus-like nanoparticles (VLPs) are icosahedral structures composed of self-assembled protein subunits with robust stability, monodisperse size and shape, genetically-controlled protein composition, and high degrees of polyvalency. Chemical functionalization of these particles[1] allows for some measure of control over their composition and function for application to a wide variety of targets.[2-5] In our own work, we have explored the cell binding abilities,[6] cellular uptake,[7] MRI imaging,[8] and plasma clearance rate[9] as a function of covalently-attached species. We describe here the pairing of such targeting techniques with the capability to produce cytotoxic species upon irradiation, for potential anticancer and other applications that require controlled killing of specific cell populations. For this proof-of-concept example, we chose to target the CD22 receptor,[10] a sugar-binding protein (lectin) that regulates certain aspects of adhesion to,[11] and cell signaling in,[12,13] B cell populations of mammalian immune systems.[14] A modified sialic acid is well known to bind selectively

CORRESPONDING AUTHOR FOOTNOTE Department of Chemistry and The Skaggs Institute for Chemical Biology, The Scripps Research Institute, 10550 North Torrey Pines Road, La Jolla, California 92037, USA. Tel: 01 858 7848845. Fax: 01 858 7848850. mgfinn@scripps.edu and Department of Molecular Chemistry and Biochemistry, Faculty of Science and Engineering, Doshisha University, Kyotanabe, Kyoto 610-0321, Japan. Tel: 081 774 65 6624. 081 774 65 6845. Fax: hkitagis@mail.doshisha.ac.jp.

SUPPORTING INFORMATION. Experimental details and additional characterization data. This material is available free of charge via the Internet at http://pubs.acs.org.

to CD22,[11,15] and we have previously constructed this molecule on a VLP surface to impart CD22 binding affinity to the particle.[6]

For cytotoxic activity, we turned to photodynamic therapy (PDT), a nonsurgical method of cancer treatment based on photosensitizer molecules that produce toxic concentrations of singlet oxygen and other reactive oxygen species upon illumination.[16] It is often desirable to locate the photosensitizer to cells of interest,[16,17] such as by covalently conjugation to cell-targeting ligands.[18,19] To enable the delivery of high local concentrations of photosensitizers, and to take advantage of polyvalent presentation of targeting groups, a wide variety of nanoparticle systems[20-22] have been explored for applications.[23,24] Francis and coworkers have recently reported an elegant light-harvesting strategy ofr porphyrin excitation using the MS2 phage particle[25] and aptamers directed against Jurkat cancer and phthalocyanines have been combined with cowpea chlorotic mottle virus capsids as well.[27]

Experimental Section

A. VLP production, purification, and analysis to verify purity, particle integrity, particle size, and protein packaging were performed as previously described.[28]

B. Syntheses. Particle **6** and compounds **3** and **4** were prepared as previously described (see Figure 1).[6] Synthetic procedures for zinc porphyrin **2** are summarized in Figure 1 and described in detail in the Supporting Information. Starting azido-triester porphyrin **A** (Figure 1) was obtained by standard Lindsey acid-mediated condensation,[29] followed by chromatographic separation.

C. Preparation of porphyrin- and glycan-decorated particles. Alkyne-derivatized Qβ (**6**) was prepared by acylation of the wild-type VLP with *N*-hydroxysuccinimide ester **5** as previously described.[30] Conjugation of all azides to **6** was performed based on the previously optimized method,[31] described briefly as follows: To solutions of **6** (2.0 mg/mL, 148 μM in protein subunit) in 0.1 M potassium phosphate at pH 7.0 were added aliquots of the stock solutions of azide-compounds (**1** in DMSO, **3** and **4** in H_2O; final concentrations: [**1**] = 100 μM for synthesis of **7**; [**1**] = 100 μM, [**4**] = 330 μM for synthesis of **9**; [**1**] = 100 μM, [**3**] = 164 μM, [**4**] = 164 μM M for synthesis of **8**). The ratio of DMSO in the aqueous reaction mixture was 2.5%. To the solution were then added a premixed solution of $CuSO_4$ with THPTA, aminoguanidine, and sodium ascorbate. The final concentrations of these reagents were [$CuSO_4$] = 0.6 mM, [THPTA] = 3.0 mM, [aminoguanidine] = 12.5 mM, and [sodium ascorbate] = 12.5 mM. After mixing, the solutions were allowed to stand at room temperature for 1 h. The resulting particles were purified by ultracentrifugation through 10-40% sucrose gradients as many times as necessary (usually twice) to provide pure material (>95% desired protein, >95% intact particles, no detectable free azides or ligand). The pellets were resuspended in 0.1 M potassium phospate at pH 7.0 or PBS to give a final protein concentration of 2.0 mg/mL. Isolated yields of purified particles **7**–**9** were >70% relative to the amount of **6** used, and loadings of the LacNAc and BPC-sialoside moieties were determined by MALDI mass spectrometry, making the assumption that coat proteins decorated with varying amounts of these small molecules are all detected with roughly the same sensitivity.

D. Cell culture. All cell culture reagents were purchased from Invitrogen, unless noted otherwise. CHO cells stably expressing human CD22 (CHO-CD22+) and Flp-In™-CHO cells (CD22-negative) were used. Cells were maintained in Dulbecco's Modified Eagle Medium: Nutrient Mixture F-12 (DMEM/F12), supplemented with 10% Newborn Calf Serum (NCS) (Omega Scientific, Inc.), 1

mM sodium pyruvate, 2.5 mM L-Glutamine, 100 units/mL penicillin, 100 μg/mL streptomycin, and either 30 μg/mL Hygromycin B (CHO-CD22+) or 25 μg/mL Zeocin (Flp-In™-CHO). Cells were grown at 37°C in a humidified 5% CO_2/95% air atmosphere. Cell concentrations were determined by the exclusion test of trypan blue using a Neubauer hemacytometer. Aliquots of 1×10^5 cells/mL were placed into 96-well dishes containing 250 μL of culture medium. The cell culture was incubated for 24 h at 37°C in a 5% CO_2 atmosphere before examination of the phototoxicity of the photosensitizer was loaded onto Qβ particles.

E. **Phase contrast and fluorescence microscopy**. Approximately 3×10^4 cells were seeded on glass coverslips and allowed to adhere for 48 hours. Qβ particles were prepared in complete growth media. Cells were rinsed once with PBS, before the addition of Qβ particles to a final concentration of 200 nM (~10^{14} particles/cell). Treated cells were then incubated at 37°C in a humidified 5% CO_2/95% air atmosphere for 4 hr. After the hour incubation period, cells were rinsed twice with PBS, and washed again two times with PBS. Images were acquired on a Nikon TE300 inverted fluorescence microscope equipped with a Roper Scientifc CoolSnap cf2 CCD camera and NIS elements software. At least 50 individual cells were examined for each experimental and control sample. Images underwent analysis and post-processing through a combination of ImageJ and Photoshop software.

F. ***In vitro*** **photobiological activity**. Qβ particles suspension was prepared in culture medium (DMEM). The cells were washed with PBS and incubated with 1 mL of buffer or solution of Qβ particles (dose = 0.05–20 nM particle; 2.5–1000 nM of zinc porphytin) at 37°C in a 5% CO_2 atmosphere for 4 h. After incubation, the cells were washed three times with PBS and fresh culture medium (1 mL) was added in each well. The wells were exposed to full spectrum or blue light (430 nm) for 90 min, with an estimated light dose of approximately 30 μwatts/cm^2 from a xenon arc lamp (Cermax LX300F). This irradiation time was chosen to produce a substantial amount of cell death at this modest light intensity. Figure S6 shows a picture of the setup, configured to avoid sample heating and to allow for filtration of the light using a narrow-bandpass filter (430±10 nm, corresponding to the porphyrin Soret absorbance). With such filtration, the light intensity reaching the sample is further reduced to a significant extent. The MTT cell viability assay was performed 24 hours later to allow the cells time to recover. When not treated with nanoparticles, the irradiation and recovery procedure resulted in no observable cellular toxicity.

Results and Discussion

To endow the icosahedral bacteriophage Qβ VLPs[32,33] with photosensitizer and targeting molecules, the zinc tetraaryl porphyrin unit, widely used for singlet oxygen generation,[18,19] was prepared with three amine-terminated hydrophilic arms (Figure 2). The resulting structure (**1**) was found to be quite water soluble and not detrimental to the protein nanparticle stability when attached. This stands in contrast to an analogous anionic porphyrin (**2**), which induced rapid decomposition of the Qβ VLP upon covalent conjugation (data not shown). For a targeting ligand, we chose the 9-biphenylcarbonyl (BPC) derivative (**3**) of the sialoside Siaα2-6Galβ1-4GlcNAc,[11,34] a potent and specific ligand for the B-cell CD22 receptor.[6,11] Compound **4**, a Galβ1,4-GlcNAc (LacNAc) disaccharide, was used as a negative control[11] for VLP modification.

Each functional molecule was synthesized with a short azide-terminated linker (see Supporting Information) to allow for VLP attachment by the highly reliable copper-catalyzed azide-alkyne cycloaddition (CuAAC) reaction,[35] assisted by accelerating ligand

THPTA.[31] Thus, the VLP, which bears a total of 720 amino groups on its surface, was acylated by a swamping concentration of *N*-hydroxysuccinimide ester **5**.[30] After purification away from the excess small molecule, the resulting poly(alkyne) particle **6** was addressed by porphyrin **1** alone (to give **7**), by a mixture of **1, 3**, and **4** (to give **8**), or by a mixture of **1** and **4** (to give negative control particle **9**). The choice to use a mixture of **3** and **4** to make the targeted particle **8** reflected an attempt to minimize non-specific adsorption to cells by covering the particle with as dense a display of glycan units as possible while avoiding the presentation of too many hydrophobic biphenyl fragments.

The resulting conjugates were characterized by MALDI mass spectrometry, which revealed complete labeling of four exposed amines per subunit (three lysines and N- terminus) for **6**, and the subsequent attachments of porphyrin and glycan azides in **7-9** (Supporting Information, Figure S2). The average loading of each species on the particle was established by the relative intensities of the corresponding peaks in the MALDI spectra, combined with measurements of Zn content to independently establish the amount of metalloporphyrin **1** attached. Size-exclusion chromatography, dynamic light scattering, and transmission electron microscopy gave data characteristic of intact monodisperse particles for **7**–**9**, as shown in the example of Figure 3b-d. The measured hydrodynamic radii of the porphyrin-bearing particles (15.3 ± 1.0 nm; Figure 3d) was slightly larger than for the non-derivatized particle (13.8 ± 0.5 nm), presumably reflecting interactions of the tethered porphyrin units with the solvent. The electronic spectrum of attached **1** showed the characteristic Soret and Q bands of a zinc tetraaryl porphyrin, along with the Qβ protein absorbance at 260 nm (Figure 3a). By comparison, the Soret band of the unattached **1** (dashed line) was broadened, presumably due to intermolecular aggregation of **1** in the aqueous buffer. Singlet oxygen generation was found to be robust by mixing the samples with singlet oxygen sensor green (SOSG) and irradiating with a filtered xenon lamp at 490 nm (Figure S4).[36,37]

Receptor- and ligand-dependent interaction with Chinese hamster ovary (CHO) cells bearing the CD22 receptor[6] was confirmed by backscattering interferometry (Supporting Information, Figure S5),[38,39] but no evidence for enhanced avidity resulting from the polyvalent display of ligand was obtained. We chose these cells for this proof-of-concept study because of their reproducible and strong overexpression of the CC22 receptor, and the ready availability of a good negative-control cell line of the same lineage but without induction of CD22 expression.

The ability of targeted particles to bind and internalize into the appropriate cells was examined using Qβ VLPs encapsulating an average of 16 copies of green fluorescent protein,[28] which were derivatized with **3** and **4** as in Figure 2. These operations did not affect the fluorescence properties of the packaged GFP, allowing us to assess binding without the potentially complicating presence of porphyrin groups on the exterior surface. (In any event, the porphyrin fluorescence was too weak to use for cellular visualization.) Incubation with CD22-negative and -positive CHO cells revealed strong binding and internalization of only the particles bearing BPC-sialoside into the cells bearing CD22 (Figure 4). Minimal interaction was observed (and has been observed before[3]) between the LacNAc-displaying particles and the CHO-CD22 cells, reflecting the low affinity of this saccharide for the receptor.[14]

Incubation of CD22-positive cells with varying concentrations of particles **8** and **9**, followed by irradiation, gave rise to dose-dependent phototoxicity as described in Figure 5. In all cases, the targeted particle **8** outperformed the nontargeted analogue **9**, but at the highest concentrations a great deal of cytotoxicity was observed for both, presumably due to nonspecific cell adsorption of **9** (Figure 5A,C). Full-spectrum xenon lamp irradiation produced more efficient cell killing activity, but also slightly lower selectivity. No

phototoxicity was observed in the presence of high concentrations of the underivatized (wild-type) particles, or of **8** in the absence of irradiation to control for possible cytotoxic effects of CD22 binding.[12] Particles **8**@GFP_{16} and **9**@GFP_{16} (Figure 4, containing GFP and simultaneously displaying porphyrin) had no greater phototoxicity effect than the corresponding particles **8** and **9** lacking the GFP chromophore. Figure 6 shows the appearance of representative samples of cells after PDT treatment, supporting the results of the MTT assay presented in Figure 5. Previously reported explorations of VLP-based photodynamic therapy were performed under somewhat different conditions (on cells immobilized on glass slides[26] and under much more intense irradiation conditions for shorter time[27]) and were quantitated in a different manner (counting stained cells in micrograph images[26,27]), making it impossible to directly compare this work with previous reports, which describe efficient and selective cell killing. However, it is clear at least that nanoparticle generators of singlet oxygen can combine targeting and cytotoxic functions in an advantageous manner.

Conclusions

The results described here highlight the modularity of multifunctional VLP-based agents, in this case allowing for cell binding and singlet oxygen generating functions to be added to an otherwise benign nanoparticle. Azide-alkyne click chemistry was used to good advantage, with efficient syntheses of each component bearing a single azide-terminated tether for attachment. An interesting dependence of particle stability on the nature of the porphyrin moiety was found, with anionic, but not cationic, substituents causing particle degradation. The ability of the BPC-sialoside ligand to selectively bind B cells[6,11,40] sets the stage for tests of these particles in the depletion of such cells *in vivo*, as a model for the treatment of certain autoimmune disorders and cancers.[15]

Supplementary Material

Refer to Web version on PubMed Central for supplementary material.

Acknowledgments

This work was supported by the NIH (CA112085 and GM60938), the W.M. Keck Foundation, and The Skaggs Institute for Chemical Biology.

References

1. Strable E, Finn MG. Curr Top Microbiol Immun. 2009; 327:1–22.
2. Uchida M, Klem MT, Allen M, Suci P, Flenniken M, Gillitzer E, Varpness Z, Liepold LO, Young M, Douglas T. Adv Mater. 2007; 19:1025–1042.
3. Flenniken ML, Uchida M, Liepold LO, Kang S, Young MJ, Douglas T. Curr Top Microbiol Immun. 2009; 327:71–93.
4. Franzen S, Lommel SA. Nanomedicine. 2009; 4:575–588. [PubMed: 19572822]
5. Steinmetz NF. Nanomedicine: nanotechnology, biology, and medicine. 2010; 6:634–641.
6. Kaltgrad E, O'Reilly MK, Liao L, Han S, Paulson J, Finn MG. J Am Chem Soc. 2008; 130:4578–4579. [PubMed: 18341338]
7. Banerjee D, Liu A, Voss N, Schmid S, Finn MG. Chembiochem. 2010; 11:1273–1279. [PubMed: 20455239]
8. Prasuhn DE J, Yeh RM, Obenaus A, Manchester M, Finn MG. Chem Commun. 2007:1269–1271.
9. Prasuhn DE Jr, Singh P, Strable E, Brown S, Manchester M, Finn MG. J Am Chem Soc. 2008; 130:1328–1334. [PubMed: 18177041]
10. Razi N, Varki A. Proc Natl Acad Sci U S A. 1998; 95:7469–7474. [PubMed: 9636173]

11. Collins BE, Blixt O, Han S, Duong B, Li H, Nathan JK, Bovin N, Paulson JC. J Immunol. 2006; 177:2994–3003. [PubMed: 16920935]
12. Haas KM, Sen S, Sanford IG, Miller AS, Poe JC, Tedder TF. J Immunol. 2006; 177:3063–3073. [PubMed: 16920943]
13. Tateno H, Li H, Schur MJ, Bovin N, Crocker PR, Wakarchuk W, Paulson JC. Mol Cell Biol. 2007; 27:5699–5710. [PubMed: 17562860]
14. Paulson JC, Chen WC, Completo GC, Macauley M, Nycholat C, Rademacher C, Rillahan C, Schwartz E, Fokin V, Nemazee D. Notes. 2010
15. Chen WC, Completo GC, Sigal DS, Crocker PR, Saven A, Paulson JC. Blood. 2010; 115:4778–4786. erratum in *Blood***2011**, *117*, 5551. [PubMed: 20181615]
16. Celli JP, Spring BQ, Rizvi I, Evans CL, Samkoe KS, Verma S, Pogue BW, Hasan T. Chem Rev. 2010; 110:2795–2838. [PubMed: 20353192]
17. Brown SB, Brown EA, Walker I. Lancet Oncol. 2004; 5:497–508. [PubMed: 15288239]
18. Hirohara S, Obata M, Alitomo H, Sharyo K, Ando T, Yano S, Tanihara M. Bioconjugate Chem. 2009; 20:944–952.
19. Chaleix V, Sol V, Huang Y-M, Guilloton M, Granet R, Blais JC, Krausz P. Eur J Org Chem. 2003:1486–1493.
20. Derycke ASL, de Witte PAM. Adv Drug Delivery Rev. 2004; 56:17–30.
21. Piao Y, Burns A, Kim J, Wiesner U, Hyeon T. Adv Funct Mat. 2008; 18:3745–3758.
22. Chouikrat R, Seve A, Vanderesse R, Benachour H, Barberi-Heyob M, Richeter S, Raehm L, Durand JO, Verelst M, Frochot C. Curr Med Chem. 2012; 19:781–792. [PubMed: 22214454]
23. Chatterjee DK, Fong LS, Zhang Y. Adv Drug Delivery Rev. 2008; 60:1627–1637.
24. Kim J, Piao Y, Hyeon T. Chem Soc Rev. 2009; 38:372–390. [PubMed: 19169455]
25. Stephanopoulos N, Carrico ZM, Francis MB. Angew Chem Int Ed. 2009; 48:9498–9502.
26. Stephanopoulos N, Tong GJ, Hsiao SC, Francis MB. ACS Nano. 2010; 4:6014–6020. [PubMed: 20863095]
27. Brasch M, De la Escosura A, Ma YJ, Uetrecht C, Heck AJ, Torres T, Cornelissen JJLM. J Am Chem Soc. 2011; 133:6878–6881. [PubMed: 21506537]
28. Rhee J-K, Hovlid M, Fiedler JD, Brown SD, Manzenrieder F, Kitagishi H, Nycholat C, Paulson JC, Finn MG. Biomacromolecules. 2011; 12:3977–3981. [PubMed: 21995513]
29. Lindsey JS, Hsu HC, Schreiman IC. Tetrahedron Lett. 1986; 27:4969–4970.
30. Udit AK, Everett C, Gale AJ, Kyle JR, Ozkan M, Finn MG. Chembiochem. 2009; 10:503–510. [PubMed: 19156786]
31. Hong V, Presolski SI, Ma C, Finn MG. Angew Chem Int Ed. 2009; 48:9879–9883.
32. Kozlovska TM, Cielens I, Dreilinna D, Dislers A, Baumanis V, Ose V, Pumpens P. Gene. 1993; 137:133–137. [PubMed: 7506687]
33. Golmohammadi R, Fridborg K, Bundule M, Valegard K, Liljas L. Structure. 1996; 4:543–554. [PubMed: 8736553]
34. Zaccai NR, Maenaka K, Maenaka T, Crocker PR, Brossmer R, Kelm S, Jones EY. Structure. 2003; 11:557–567. [PubMed: 12737821]
35. Rostovtsev VV, Green LG, Fokin VV, Sharpless KB. Angew Chem Int Ed. 2002; 41:2596–2599.
36. Zhu Z, Tang Z, Phillips JA, Yang R, Wang H, Tan W. J Am Chem Soc. 2008; 130:10856–10857. [PubMed: 18661988]
37. Dimitrijevic NM, Rozhkova E, Rajh T. J Am Chem Soc. 2009; 131:2893–2899. [PubMed: 19209860]
38. Baksh MM, Kussrow A, Mileni M, Finn MG, Bornhop DJ. Nature Biotechnol. 2011; 29:357–360. [PubMed: 21399645]
39. Bornhop DJ, Latham JC, Kussrow A, Markov DA, Jones RD, Sorensen HS. Science. 2007; 317:1732–1736. [PubMed: 17885132]
40. Duong BH, Tian H, Ota T, Completo GC, Han S, Vela JL, Ota M, Kubitz M, Bovin N, Paulson JC, Nemazee D. J Exp Med. 2010; 207:173–187. [PubMed: 20038598]

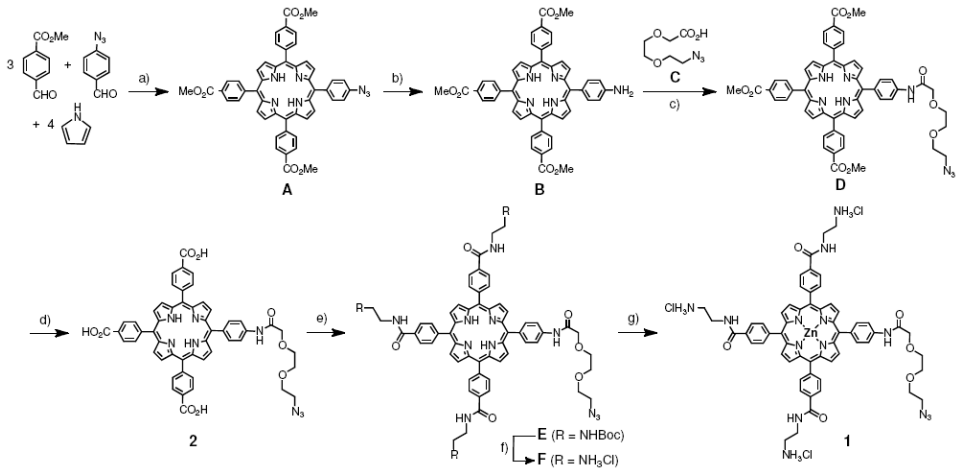

Figure 1.

Synthesis of azide-tailed porphyrins. a) BF_3•Et_2O, CH_2Cl_2, 8%; b) Na_2S, CH_3Cl/MeOH, reflux, 70%; c) EDC, HOBt, Et_3N, CH_2Cl_2, 74%; d) NaOH, H_2O, THF, 96%; e) $BocNH(CH_2)_2NH_2$, EDC, HOBt, Et_3N, DMF, 54%; f) TFA, CH_2Cl_2, ion exchange (Cl^- form), 90%; g) ZnO, H_2O/MeOH, 86%.

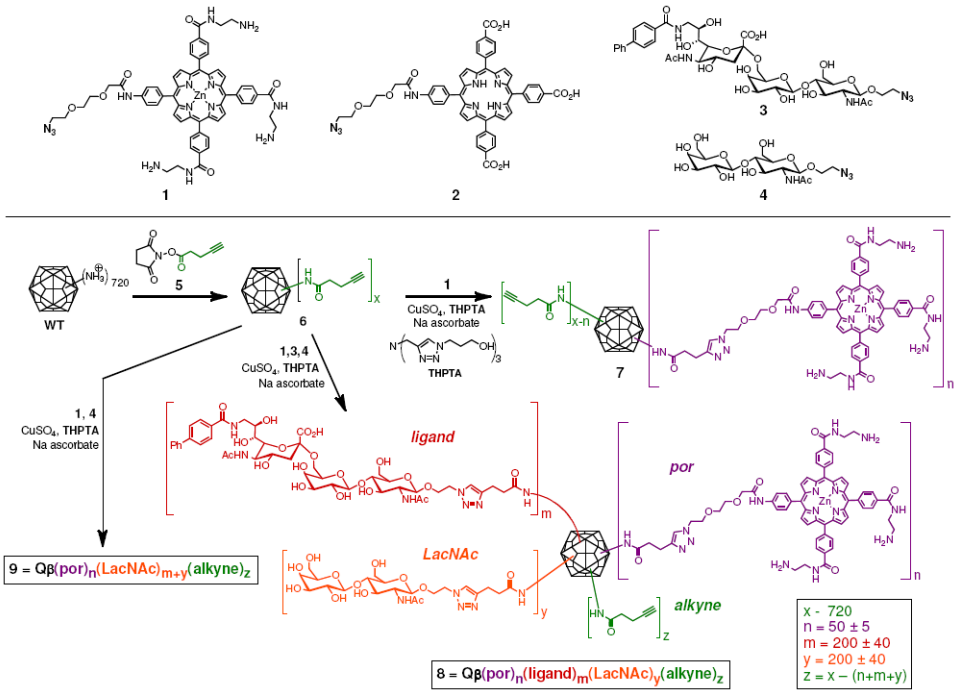

Figure 2.
Surface functionalization of Qβ VLPs for tests of singlet oxygen generation and cell phototoxicity.

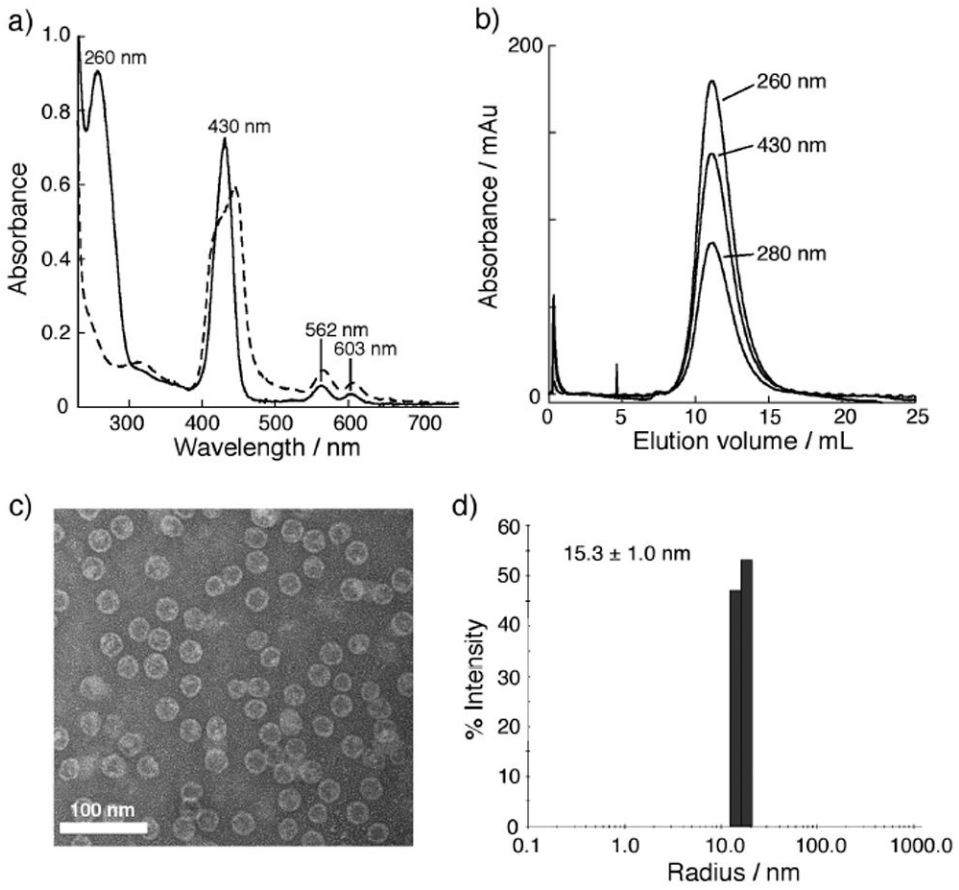

Figure 3.

Characterization of particle **7**. (a) UV-vis absorbance spectra for **7** (solid line) and **1** (dashed line) in buffer, pH 7.4. (b) Size-exclusion FPLC showing co-elution of porphyrin with particle, verifying their covalent linkage. (c) Negative-stain transmission electron microscopy. (d) Dynamic light scattering determination of hydrodynamic radius. The corresponding data for **8** and **9** are very similar.

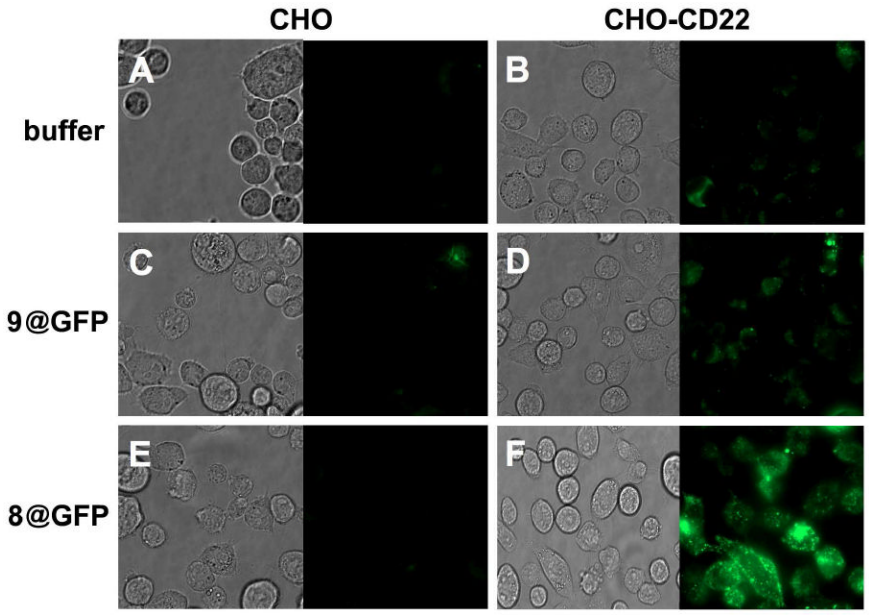

Figure 4.

Phase contrast and fluorescent microscope images of CHO (A, C and E) and CHO-CD22+ cells (B, D and F) incubated with PBS (A and B), **9**@GFP_{16} (C and D), and **8**@GFP_{16} (E and F) at 37 °C for 4 hours. Each particle was used at 1 nM (50 nM in porphyrin); the @ symbol denotes the encapsidation of multiple copies of GFP inside the particle. The faint signals observed in panels A and B are due to cellular autofluorescence.

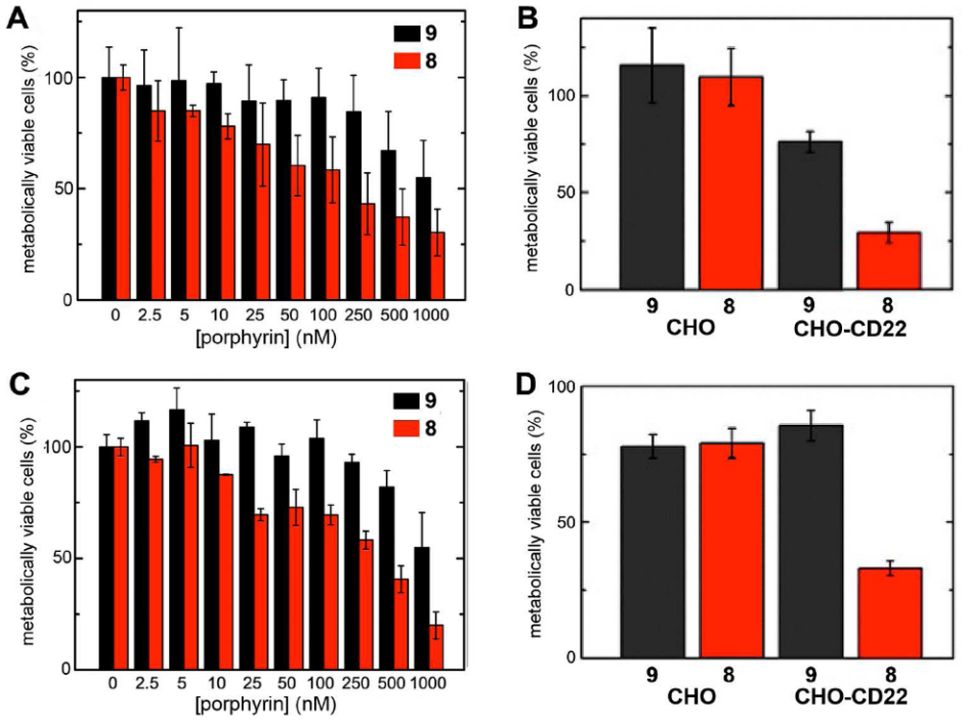

Figure 5.

(A) Dose-response phototoxicity induced by zinc porphyrin-loaded Qβ particles on CHO-CD22 cells, under full-spectrum irradiation (IC_{50} ≈ 80 nM in porphyrin, 1.6 nM in particle); (C) Same as A, but with filtered irradiation (430±10 nm, IC_{50} ≈ 230 nM in porphyrin, 4.6 nM in particle). (B) Comparison of CD22-negative and −positive cells at 10 nM particle concentration (0.5 μM in porphyrin), under full-spectrum irradiation. (D) As in B, but with 50 nM particles (2.5 μM in porphyrin), under irradiation at 430±10 nm. For all panels, cells were incubated with the indicated particles at 37°C. for 4 h, washed, and irradiated for 90 min using a custom-built xenon lamp assembly (Figure S6). The MTT assay was performed 24 h after light exposure.

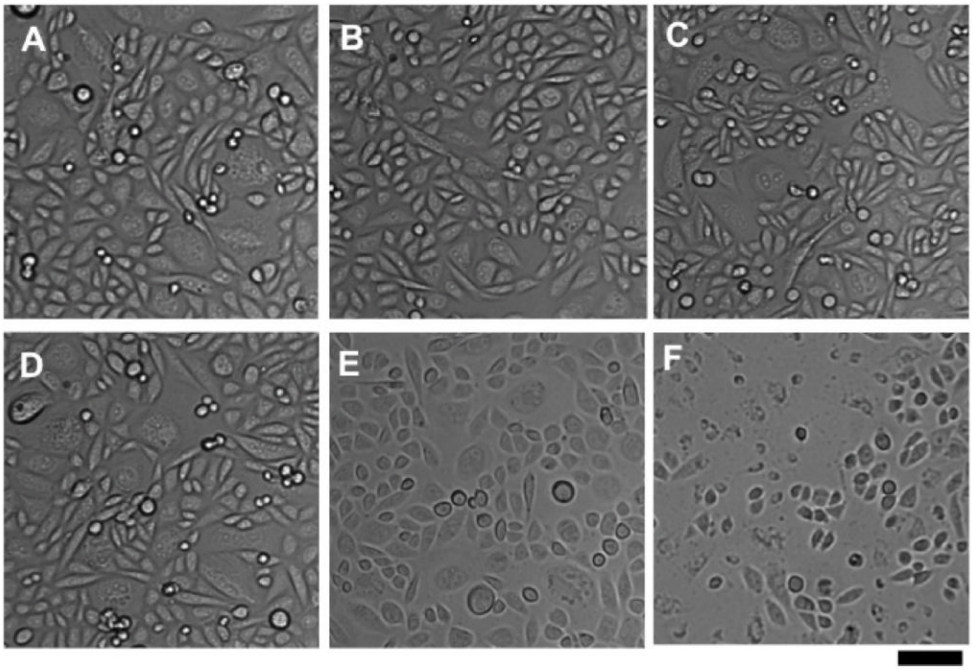

Figure 6.

Phase contrast microscopy of CHO-CD22 cells after treatment with particles and light as described in Figure 5. (A-C) Cells incubated with LacNAc-loaded Qβ particles **9**. (D-F) Cells incubated with BPC ligand-loaded Qβ particles **8**. (A,D) Cells incubated with 10 nM particle for 4 h at 37°C. (B,E) After incubation with particle, washing, and irradiation (430 ± 10 nm, 90 min, RT). (C,F) After incubation with particle, washing, irradiation, incubation in CO_2 incubator overnight at 37°C. Scale bar = 50 μm.